Journal of Building Engineering 87 (2024) 108960

Contents lists available at ScienceDirect

Journal of Building Engineering

journal homepage: www.elsevier.com/locate/jobe

Design automation of sustainable self-compacting concrete containing fly ash via data driven performance prediction

Tianyi Cui, Sivakumar Kulasegaram *, Haijiang Li

School of Engineering, Cardiff University, Cardiff, CF24 3AA, UK

ARTICLE INFO

Keywords:
Machine learning
Self-compacting concrete
Random forest
Support vector machine
Decision tree
Artificial neural network

ABSTRACT

Self-compacting concrete (SCC) is a highly flowable and segregation-resistant material, effectively facilitating proper filling and ensuring exceptional structural performance in confined spaces. Incorporating fly ash as a supplementary cementitious material in SCC mixtures yields numerous benefits, including enhanced cost-effectiveness in construction and the advancement of environmental sustainability. Nevertheless, the addition of fly ash in SCC poses significant challenges in modelling and predicting the properties of SCC due to lack of understanding of its influence on material rheology and bonding. It is therefore desirable to develop more appropriate machine learning approach to compliment the large scale and costly laboratory-based experiments. This paper presents four well trained supervised machine learning models for the prediction of fresh and hardened properties of SCC containing fly ash: support vector machine (SVM), decision tree, random forest, and artificial neural network (ANN). Training datasets gathered from publicly available existing relevant literature, were analysed and processed prior to shape the required machine learning models. Optimization strategies of hyperparameters were also implemented for each model. To evaluate the performance of these machine learning models and to compare their accuracy, regression error characteristic curves and Taylor diagrams were utilized. The findings reveal that all models demonstrate promising results, with the random forest model outperforming the others in predicting SCC properties with higher accuracy. This underscores the potential of random forest algorithms in accurately modelling and predicting the properties of fly ash-infused SCC. Finally, a data driven implementation framework has been developed, thereby offering robust and logical strategy for experimental designs and guidance for developing sustainable SCC.

1. Introduction

Concrete is an essential construction material that plays a vital role in the development and advancement of modern society. Self-compacting concrete (SCC), firstly proposed by Okamura and Ozawa in 1996 [1], has emerged as a promising alternative to traditional concrete due to its unique properties and characteristics. SCC is a highly flowable and good segregation resistant material that can be easily placed and compacted without the need for any external vibration [2]. This excellent feature of SCC makes it highly efficient and reliable, especially in applications where traditional concrete placement methods are difficult or impossible to implement. The development and application of SCC have been a significant research focus in the field of construction materials in recent years, with a wide range of studies have been conducted to explore its properties and behaviour [3–7].

* Corresponding author.
E-mail address: kulasegarams@cardiff.ac.uk (S. Kulasegaram).

https://doi.org/10.1016/j.jobe.2024.108960
Received 2 December 2023; Received in revised form 9 February 2024; Accepted 28 February 2024
Available online 7 March 2024

SCC offers significant advantages over traditional vibrated concrete in terms of reducing construction costs and improving the construction environment, making it an important step towards sustainable concrete [8]. However, the current technology for the production of SCC often requires a higher volume of binder materials. This increase in binder materials not only results in higher production costs but also significantly increases the environmental impact including sustainability [9]. Hence, numerous researchers have investigated the incorporation of supplementary materials to SCC to reduce the cost and to increase its resistance to environmental degradation. Fly ash, ground granulated blast furnace slag (GGBS), silica fume and other supplementary materials (SCMs) have

Table 1
Summary of research on the prediction of SCC properties based on machine learning models.

Ref.	Year	Algorithms used	Notation	Dataset	Input variables	Output variables
[23]	2011	Artificial neural network	ANN-I	80	Cement, water/powder, FA, CA, SP, fly ash	Compressive strength
			ANN-II	31	Cement, water, water/powder, SP, FA, CA, bottom ash, fly ash	Compressive strength
[24]	2016	Artificial neural network	ANN	169	Cement, water, FA, CA, RHA, SP, VMA, limestone powder, fly ash, GGBS, silica fume	Compressive strength
[25]	2016	Biogeographical-based programming	BBP	413	Compressive strength	Elastic modulus
		Artificial bee colony programming	ABCP			
[26]	2017	Artificial neural network	ANN	114	Binder, water/binder, FA, CA, SP, fly ash percentage	Compressive strength, slump diameter, V-funnel time, L-box ratio
[27]	2018	Decision tree	DT	114	Binder, water/binder, FA, CA, SP, fly ash	Compressive strength, slump diameter, V-funnel time, L-box ratio
[28]	2019	Artificial neural network	ANN	205	Cement, water, FA, CA, RHA, SP, VMA, limestone powder, fly ash, GGBS, silica fume	Compressive strength
[29]	2020	Support vector machines	SVM	115	Binder, water/powder, FA, CA, SP, fly ash	Compressive strength, slump diameter, V-funnel time, L-box ratio
[30]	2020	Support vector machines	SVM	340	Cement, water/cement, water/powder, water/binder, FA/powder, CA/powder, HWR/powder, VMA/powder, fly ash/binder, microsilica/binder	Compressive strength, slump diameter, V-funnel time, orimet, U-box and L-box ratio
[31]	2020	Multivariate Adaptive Regression spline	MARS	360	Fly ash/binder, silica fume/binder, temperature	Rapid chloride permeability
		Minimax Probability Machine Regression	MPMR			
[32]	2021	Artificial neural network	ANN	300	Cement, water/binder, FA, CA, SP, fly ash	Compressive strength
		Support vector machine	SVM			
		Gene expression programming	GEP			
[33]	2021	Artificial neural network	ANN	366	Binder, water/binder, FA, CA, SP, age, silica fume	Compressive strength
[34]	2021	Artificial neural network	ANN	327	Cement, water, FA, CA, SP, age, fly ash	Compressive strength
		Radial basis function neural network	RBFNN			
		Firefly optimization algorithm	FOA			
		Hybrid model				
[35]	2022	Multiple Linear Regression	MLR	100	Water absorption, void ratio, sonic velocity at 1 day and 7 days, compressive strength at 1 day and 7 days	Compressive strength
		Random Forest	RF			
		Decision Tree	DT			
		Support vector machines	SVM			
[36]	2022	Multivariable regression model	MRM	59	Slump flow diameter, V-funnel time, L-box ratio	Yield stress, viscosity
		Artificial neural network	ANN			
[37]	2022	Nine ensemble models		515	Cement, water, FA, CA, SP, Mineral admixture	Compressive strength
		Two generalized additive model	GAM			
[38]	2022	Artificial neural network	ANN	85	Cement, water/binder, FA, CA, SP, fly ash, silica fume	Compressive strength
		Support vector machines	SVM			
[39]	2022	Artificial neural network	ANN	400	Cement, water/binder, FA, CA, recycled plastic aggregate, SP, age, fly ash, silica fume, limestone powder, GGBS	Compressive strength

been extensively studied for their potential to enhance the properties of SCC [10–15]. The addition of such materials in concrete, particularly SCC mixtures, presents significant challenges in accurately estimating concrete properties due to the highly nonhomogeneous mixture with various constituents. Accordingly, it is essential to develop reliable predictive models to reduce the cost of conducting more experiments.

The main objective of the present study is to propose a highly efficient implementation of machine learning models on predicting fresh and hardened properties of SCC containing fly ash. For evaluating fresh properties, the yield stress is assessed using the slump flow test, while the plastic viscosity is determined by the V-funnel time [16]. In this work, four machine learning algorithms, namely support vector machine (SVM), decision tree (DT), random forest (RF) and artificial neural network (ANN), were developed and compared via regression error characteristic curves and Taylor diagrams. Moreover, the data processing strategies and the optimal hyperparameter selection were also investigated in this paper. This work aims to devise machine learning models addressing the stated issues through two key avenues:

1) Innovating and delving into the parameter optimization strategies, emphasizing the examination and comparison of the effectiveness of diverse algorithms.
2) Assessing the precision of the predicted fresh and hardened properties of SCC by the developed framework.

The outline of remaining sections of this study is as follows: Section 2 gives a general literature review on four machine learning algorithms. Section 3 presents an overview of the methodology. Section 4 elaborates on the dataset and the steps taken for data preprocessing. Section 5 of this study presents a detailed discussion on the development and evaluation of predictive models for fresh and hardened properties of SCC with fly ash. Additionally, an in-depth analysis of hyperparameter selection and related comparative analysis is also presented in this section. Subsequently, a data driven framework is established to foster additional research and exploration. Furthermore, the limitations of this study are also highlighted. The concluding remarks are summarized in Section 6.

2. Literature review

With the development of big data processing techniques and the continuous improvement of computer performance, machine learning technology has been widely used in various fields such as data mining, natural language processing, etc. However, the technology is in its early stages of implementation in the construction industry. With regards to the prediction of concrete properties, smart computing algorithms are utilized in the aim of achieving greater accuracy by minimizing the error between predicted results and data obtained from experiments or literature [17]. Young et al. [18] presented statistical and machine learning models to estimate the compressive strength based on concrete proportions in which a large dataset was taken into account. Subsequently, the predictive models were utilized to design concrete mixtures that are optimal in terms of both cost and environmental impact. Sun et al. [19] utilized a laboratory-prepared specimen to propose an evolved support vector regression tuned by antennae search, which predicted the permeability and unconfined compressive strength of pervious concrete. In the neural network model proposed by Behnood et al. [20], the tensile strength of steel fibre-reinforced concrete (SFRC) was predicted using compressive strength as an input variable. Recently, ensemble methods have also been developed and employed to predict concrete properties using various algorithms. Asteris et al. [21] proposed a hybrid ensemble model that utilizes four conventional machine learning algorithms to predict the compressive strength of concrete. The proposed model was demonstrated to achieve higher predictive accuracy compared to the individual models.

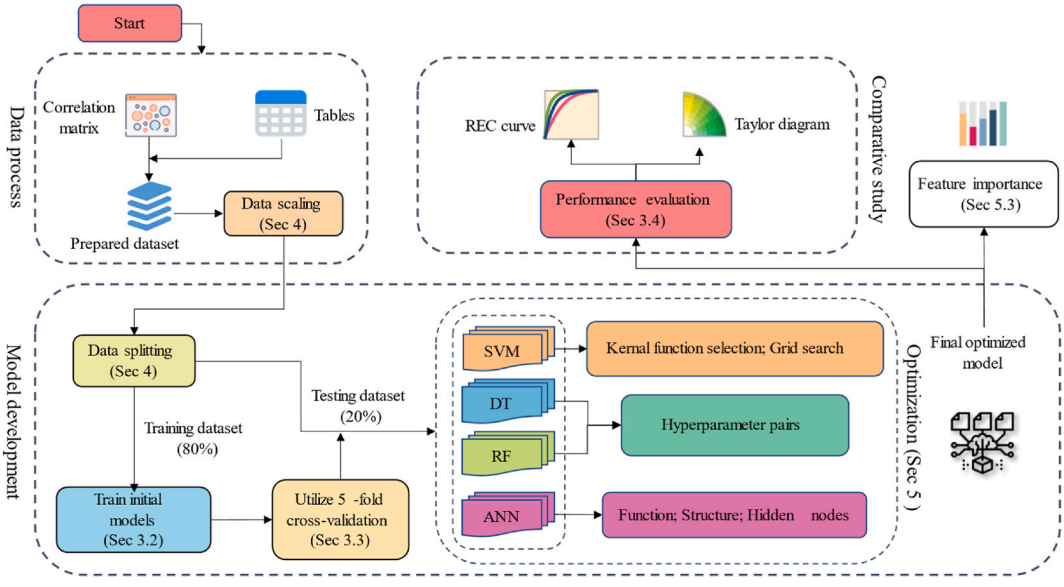

Fig. 1. Flowchart of the presented data driven framework for the prediction of the SCC properties.

Nafees et al. [22] predicted the compressive strength of silica fume-based concrete based on six main input factors. In their study, the ensemble models showed a great improvement on the prediction efficiency.

The popularity of SCC has grown significantly due to its excellent performance in terms of workability and mechanical properties. As a result, several studies have been conducted to predict the properties of SCC in recent years. Table 1 outlines some recent studies that adopted various machine learning algorithms for accessing SCC properties, along with the datasets and variables employed in each study. It is evident that the majority of the research has focused on developing prediction models based on the content of the primary SCC ingredients and the substitution level of SCMs. As an efficient machine learning algorithm, artificial neural network-based methods have gained more popularity among all others. It can also be noted that some researchers have studied the predictive performance of single machine learning models on the fresh properties of SCC.

3. Methodology

Machine learning, fundamentally a data driven approach, refers to statistical approaches for data analysis and is commonly employed for tasks such as data classification and regression analysis. This section summarises the presented machine learning framework based on four basic algorithms integrating multiple innovative techniques. Performance metrics are defined to establish the validity of the proposed models on the prediction of SCC properties.

3.1. Overview

Fig. 1 shows the flowchart of the proposed framework with main factors considered in this paper. The primary steps are as follows: (1) Three groups of datasets are established, taking into account the most influential variables on SCC properties from the literature focused on SCC with fly ash. (2) The datasets are scaled and randomly split into training and testing tests. Section 4 presents the statistical analysis and preparation of datasets. (3) Initial models are developed based on the datasets. (4) Various hyperparameter optimization strategies based on five-fold cross-validation for each model are explored. Section 3.2 and 3.3 detail the model development, optimization methods and the cross-validation method, respectively. This process is presented in Section 5.1. (5) The predictive models are evaluated using various performance metrics as defined in Section 3.4. (6) A comparative study is performed for the optimized models, with results presented via REC curves and Taylor diagrams. The best-performing machine learning models for predicting SCC properties with fly ash are identified based on the comparative study, as discussed in Section 5.2. (7) The impact of mix ingredients on the fresh and hardened properties of SCC is investigated in Section 5.3. (8) Potential implementation on the proposed data driven framework is developed in Section 5.4.

3.2. Initial and optimized strategies for machine learning models

Support vector machines (SVMs), originally developed by Vapnik and his colleagues [40–42] in the 1900s, have undergone significant expansion and are widely applied in the domains of computer vision and data mining. The learning strategy of SVM focuses on margin maximization, which ultimately resolves into a convex quadratic programming problem [43]. To tackle the challenge of separating the nonlinear data that cannot be effectively separated within a 2D plane, linear inseparable data is mapped into a higher dimensional space through a kernel function [44]. To improve the estimation accuracy and generalization ability of SVM models,

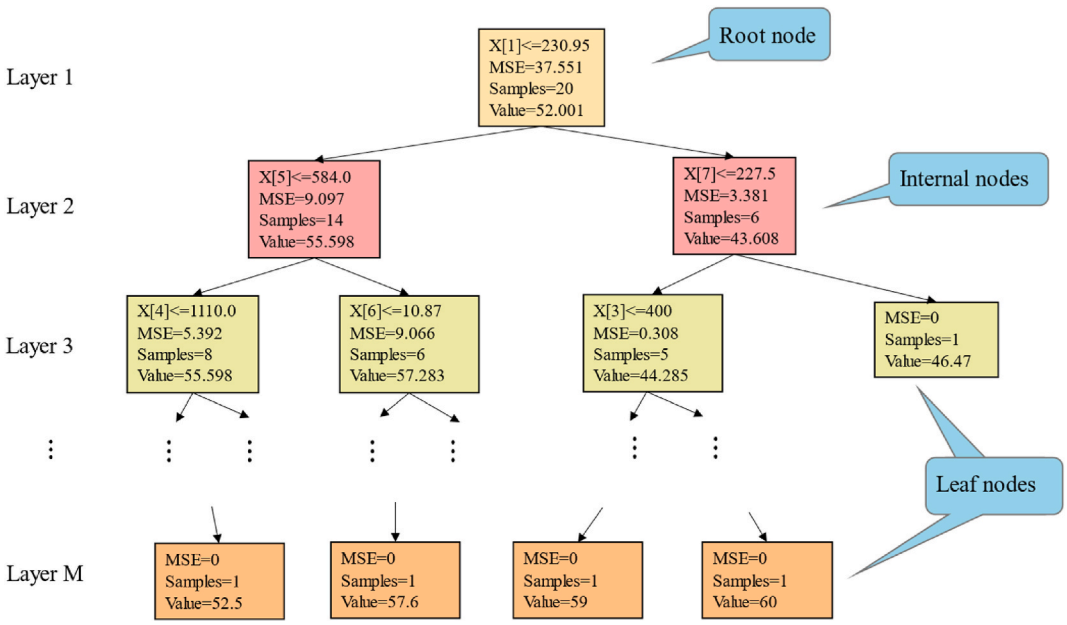

Fig. 2. The representative structure of a CART decision tree.

consideration of parameter settings is required. The penalty parameter, C, is used to control the trade-off between the ability of the model to generalize and its performance on the test dataset. A larger value of C decreases the margin and potentially overfits the model. Hyperparameter optimization greatly benefits from cross-validation based grid search.

The decision tree (DT) employs a top-down recursive learning approach. The fundamental concept is to construct a tree that exhibits the fastest entropy reduction, eventually reaching a leaf node with zero entropy. To enhance predictive accuracy of the decision tree, it is crucial to determine an appropriate impurity splitting criterion, which guides feature selection and partitions at each internal node. The prediction of numerical outcomes based on input variables predominantly utilizes four decision tree algorithms: CHAID (Chi-squared automatic interaction detection), CART (classification and regression trees), C4.5, and C5.0 [45]. In CART, each non-leaf node in the tree branches into two child nodes. Fig. 2 illustrates an exemplary structure of a CART decision tree, as employed in this study. This visual representation highlights the binary branching nature of the algorithm and the decision-making process at each internal node. To address the overfitting issue, the tree-based ensemble learning algorithm, random forest (RF), has been introduced for predicting SCC mixes. By leveraging the combined strength of multiple decision trees, random forest improves generalization performance while reducing the risk of overfitting.

A typical artificial neural network (ANN) comprises three primary components: structure, activation functions, and learning rules. The structure specifies the variables and their topological relationships in the network. Generally, an ANN consists of the input layer, one or more hidden layers, and an output layer, which enable the processing and transformation of input data into meaningful predictions or classifications. The activation function, usually a nonlinear function, determines the rules governing the ways that dictate the modification of neuron activation values based on the activity of other neurons in the network. This nonlinearity enables the ANN to capture and model complex relationships in the data, thereby enhancing its predictive capabilities [46]. Learning rules decide the change of weights between neurons over time, enabling the network to improve its performance as it processes more data. This study employs the back-propagation neural network (BPNN), a multi-layer feedforward network. In practice, the number of the hidden layers and the number of nodes in the hidden layer are dictated by the collected dataset and its features [47]. The selection of the number of hidden nodes was a significant focus of investigation in this study.

3.3. Five-fold cross-validation

In the actual training process, the trained model usually behaves well to the training datasets while responds poorly when new datasets are provided. Cross-validation is a commonly used method in machine learning for building models and verifying model parameters [48]. It aims to improve the generalization ability of the model by dividing the sample datasets and combining them into different training and testing sets. In addition, the limited amount of available data can be reused to improve the modelling efficiency [49]. Therefore, the five-fold cross validation was employed in this study, and the steps are shown as following.

Step 1. Randomly divide all datasets into 5 subsets by sampling without repetition.

Step 2. Train the model by using 4 of the 5 subsets and the remaining 1 subset is used for testing.

Step 3. Repeat the previous step five time to ensure each subset is used once as the test set.

Step 4. Save the evaluation index of all five models.

Step 5. Calculate the mean error of the test results of 5 models as the cross-validation error.

All steps of the model training process, including model selection and feature selection, are performed independently within a single 'fold'. The schematic description of five-fold cross-validation is presented in Fig. 3.

3.4. Model performance evaluation

The performance of fully developed models in predicting SCC mix properties is quantified using four statistical measures. The

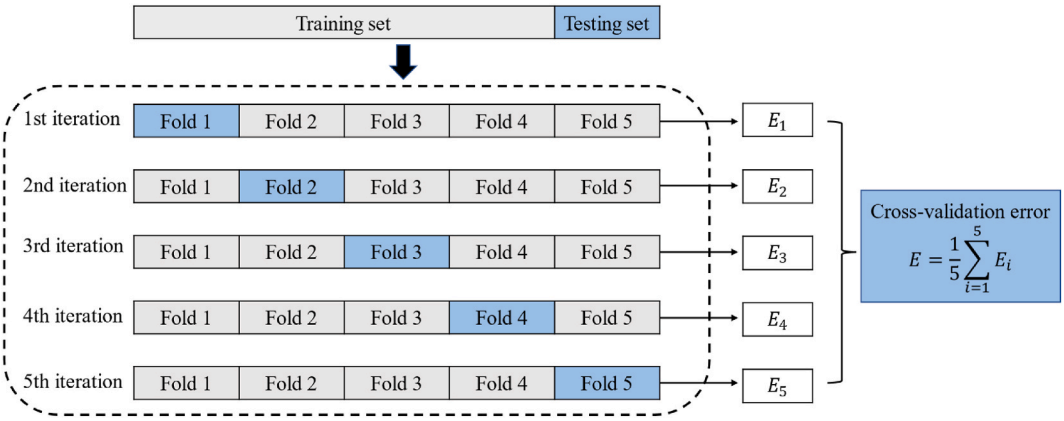

Fig. 3. The schematic structure of five-fold cross-validation.

accuracy indicators employed in this study are correlation coefficient (R), coefficient of determination (R^2), mean absolute error (*MAE*), and root mean squared error (*RMSE*). The mathematical expressions are given in Equations (1)–(4).

$$R = \frac{\sum_{i=1}^{N}(P_i - P_A)(E_i - E_A)}{\sqrt{\sum_{i=1}^{N}(P_i - P_A)^2 \sum_{i=1}^{N}(E_i - E_A)^2}} \tag{1}$$

$$R^2 = 1 - \frac{\sum_{i=1}^{N}(P_i - E_i)^2}{\sum_{i=1}^{N}(E_i - E_A)^2} \tag{2}$$

$$MAE = \frac{1}{N}\sum_{i=1}^{N}|P_i - E_i| \tag{3}$$

$$RMSE = \sqrt{\frac{1}{N}\sum_{i=1}^{N}(P_i - E_i)^2} \tag{4}$$

To demonstrate higher accuracy, R and R^2 values should be closer to 1, indicating a strong correlation between the predicted and experimental values and signifying that they tend to vary in a similar manner. The values of *MAE* and *RMSE* are the measurements of the difference, near to zero means greater accurate, as they indicate smaller deviations between the predictions and the actual data.

4. Data process and parameters

This study aims to predict both fresh and hardened properties of SCC mixes containing fly ash. Many previous studies had focused mainly on assessing a single output characteristic based on a series of input variables. This study considers three output variables to achieve a more comprehensive forecast. Considering the database from the published literature, the properties of SCC mix design, including compressive strength (*Fcu*) of 501 mixes [3,11,50–74], slump flow diameter (*SD*) of 217 mixes [2,11,51–66,70–73,75,76] and V-funnel time (*VF*) of 144 mixes [11,51–64,66,72,75,76], were collected to evaluate the properties of SCC containing fly ash, by utilizing the machine learning modelling. The input variables encompass the amount of cement (C), fly ash(F), water to binder ratio (W/B), fine aggregates (FA), coarse aggregates (CA), superplasticizers (SP) and curing age, with the age being employed exclusively for compressive strength prediction. The relationships representing the SCC properties are expressed by Equations (5)–(7).

$$Fcu, (MPa) = f_1(C, F, W/B, FA, CA, SP, Age) \tag{5}$$

Table 2
Statistical analysis on collected datasets.

Variables	Symbol	Unit	Category	Min	Max	Average	Standard deviation	Count
Dataset 1: SCC compressive strength (501 samples)								
Cement	C	kg/m^3	Input	100	670	350	119	501
Water to binder ratio	W/B	–	Input	0.26	0.70	0.39	0.08	501
Fly ash	F	kg/m^3	Input	0	428	145	95	501
Fine aggregate	FA	kg/m^3	Input	369	1180	828	147	501
Coarse aggregate	CA	kg/m^3	Input	455	1085	790	137	501
Superplasticizer	SP	kg/m^3	Input	0.78	21.84	5.15	4.35	501
Curing age	Age	days	Input	1	720	47	82	501
Compressive strength	Fcu	MPa	Output	0.36	105.88	42.14	20.38	501
Dataset 2: SCC slump flow (217 **samples)**								
Cement	C	kg/m^3	Input	0	670	359	114	217
Water to binder ratio	W/B	–	Input	0.26	0.70	0.37	0.08	217
Fly ash	F	kg/m^3	Input	0	439	170	98	217
Fine aggregate	FA	kg/m^3	Input	369	1180	837	123	217
Coarse aggregate	CA	kg/m^3	Input	455	1085	740	124	217
Superplasticizer	SP	kg/m^3	Input	0.78	21.84	5.52	4.41	217
Slump flow diameter	SD	mm	Output	555	830	712	58	217
Dataset 3: SCC V-funnel (144 **samples)**								
Cement	C	kg/m^3	Input	0	670	367	126	144
Water to binder ratio	W/B	–	Input	0.26	0.70	0.38	0.09	144
Fly ash	F	kg/m^3	Input	0	439	146	103	144
Fine aggregate	FA	kg/m^3	Input	369	1180	820	145	144
Coarse aggregate	CA	kg/m^3	Input	533	944	763	103	144
Superplasticizer	SP	kg/m^3	Input	0.78	21.84	6.23	5.17	144
V-funnel time	VF	sec	Output	1.31	22.00	7.29	3.32	144

$$SD, (mm) = f_2(C, F, W/B, FA, CA, SP) \tag{6}$$

$$VF, (s) = f_3(C, F, W/B, FA, CA, SP) \tag{7}$$

The statistical results which were summarized and calculated from collected datasets are presented in Table 2. For the purpose of improving the accuracy of comprehensive predictions in SCC properties, the key variables have been confined within a consistent range. For instance, the W/B is set between 0.26 and 0.7, while the range for SP is established between 0.78 kg/m^3 and 21.84 kg/m^3. It can be seen that the dataset is complete and the handling on missing data is not required in this case. In order to reveal more information and to analyse the relationship between all input and output variables, the correlations of variables are provided. For this purpose, the Pearson's correlation coefficient is used in this study as shown in Equation (1). The range of coefficient are limited to −1 to +1 as ensured by the formulation. The value close to 0 indicates weak relationship between variables. It should be noted that this coefficient can only measure the linear correlation between variables [77]. This means even though the coefficient is close to 0, it cannot be concluded that there is no other relationship between quantities. Fig. 4 displays the heatmaps illustrating the correlations between features within the datasets. There is a significant relationship between fly ash content and cement with correlation coefficient of −0.8, −0.78 and −0.82, respectively. On the contrary, the correlation between superplasticizer and components of SCC mixtures is quite weak in Dataset 1 (in Table 2), which is consistent with reality.

In order to evaluate the generalization error of the predictive models, each dataset was randomly split into two groups in this study. The training sets, which is 80% of all data points, were used for building machine learning models. The remaining 20% were used for testing the trained models. For example, in the case of Dataset 1, 400 groups of measurements were used as training set and 101 measurements were used for the assessment of models. To eliminate the error caused by units and ranges of all variables, it is necessary to process datasets after the data splitting. It has been proven that scaling increases the speed in obtaining the optimal solution in some algorithms and also improves the accuracy of prediction [78]. In this study, the Standard Scaler function in scikit-learn library was employed.

5. Results and discussion

5.1. Determination of optimized machine learning models

The compressive strength and fresh properties of SCC were predicted in this section via four machine learning algorithms which include SVM, decision tree, random forest and ANN. The training of models was implemented in MATLAB and PYTHON 3.6, utilizing essential libraries such as Scikit-learn, NumPy, Pandas, Matplotlib, and Seaborn. In addition to proposing parameter optimization strategies, these strategies were diligently applied within this section. These tactics were intricately executed to fine-tune the performance of models, playing a crucial role in enhancing the overall quality of prediction outcomes.

5.1.1. Prediction of SVM model

As the SVM algorithm employs the Euclidean distance of the sample data, it is essential to standardize the input and output datasets to prevent data with larger values from dominating the model. Standardization involves transforming all data into a normal distribution with a mean value of 0 and a variance of 1, thereby ensuring a more balanced representation of the data within the algorithm. The selection of kernel function typically relies on domain-specific knowledge, as well as the number of samples and feature variables in the dataset [79]. In this study, four commonly used kernel functions were investigated, encompassing Linear, Polynomial (Poly), Radial basis (RBF), and Sigmoid functions. Table 3 shows the performance of each kernel function for the corresponding output variables in different predictive models.

To mitigate the impact of random grouping of training and testing datasets in programming, the random state was set to the optimal fixed value obtained by looping. As can be seen, the RBF kernel function performed the best for all output parameters, exhibiting the highest R^2 values and the lowest errors. Indeed, the R^2 values being less than 0.9, along with relatively high RMSE and MAE values, suggest that while the RBF kernel function outperforms the other kernel functions considered, there is still potential for enhancing the predictive capabilities of models. It should be noticed that the R^2 values for the sigmoid function obtained using Scikit-learn Library are

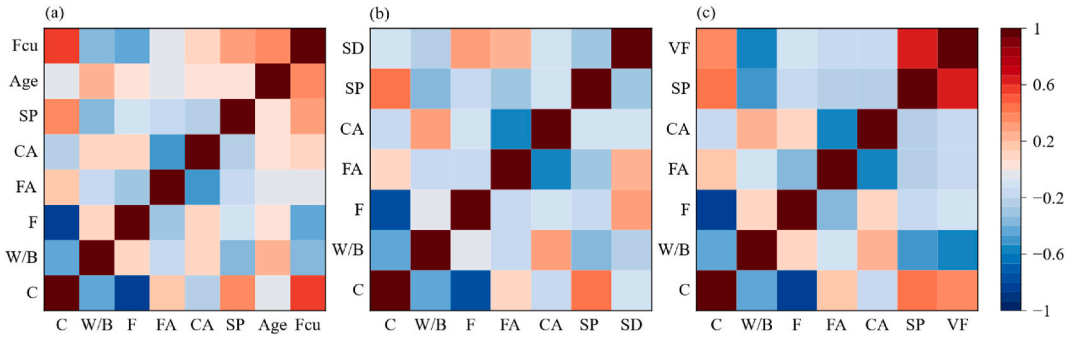

Fig. 4. Correlation matrix of variables for predicting (a) compressive strength, (b) slump flow, (c) V-funnel time.

Table 3
Statistical results of initial SVM models with various kernel functions.

Output variable	Kernel function	Statistical parameters		
		R^2	RMSE	MAE
Fcu	Linear SVM	0.634	12.480	10.002
	Poly SVM	0.636	12.452	9.322
	RBF SVM	**0.860**	**7.721**	**5.847**
	Sigmoid SVM	−24.609	104.447	72.941
SD	Linear SVM	0.578	35.601	28.937
	Poly SVM	0.636	33.078	26.263
	RBF SVM	**0.733**	**28.320**	**21.918**
	Sigmoid SVM	−6.533	150.389	111.121
VF	Linear SVM	0.810	1.352	1.064
	Poly SVM	0.444	2.314	1.908
	RBF SVM	**0.860**	**1.162**	**0.990**
	Sigmoid SVM	−1.149	4.549	3.769

less than zero in some models. This indicates that the prediction error of the fitted function is greater than that of a simple mean - value function [80]. In other words, the inferior performance of the sigmoid kernel function, when compared to a model that predicts only the average value of the output, indicates that it is not an appropriate choice for this specific problem domain. In summary, the effective RBF kernel was selected for the subsequent model optimization and performance evaluation.

There are two main factors that need to be set for the RBF kernel function which are parameters *C* and *gamma*. The selection of optimal parameters significantly affects the accuracy of an SVM model [44,81]. The cross-validation based grid search technique was utilized to find the optimal parameter pairs of *C* and *gamma*. The steps involved in this process are summarized as follows:

Step 1. Set $C \in [2^{-5}, 2^{15}]$ and $gamma \in [2^{-15}, 2^{3}]$. This range of values for *C* and *gamma* provides a comprehensive search space to find the optimal parameters in this study [81].

Step 2. Obtain a 20×18 coarse grid within the specific range of values for *C* and *gamma*.

Step 3. Perform five-fold cross-validation for the parameter pair corresponding to the first point in the grid and calculate five *MAE* values. Then, compute the average of these *MAE* values as the representative score for this particular point.

Step 4. Traverse all points in the grid and repeat Step 3 for each point to calculate the corresponding *MAE* values, identifying the best parameter pair that yields the lowest error.

The graphs of parameter optimization results are shown in Fig. 5. After setting the optimal values of RBF kernel parameters, new models were trained and tested using the same random states for data splitting and cross-validation. Table 4 presents the best parameter pairs and performance of the developed SVM models for predicting the compressive strength, slump flow diameter and V-funnel time. It can be observed that the optimized SVM with selected kernel parameters showed highest accuracy in estimating compressive strength of SCC mixes. The average *MAE* value obtained during the parameter selection process was used to evaluate the performance of the models during the training phase. As determined by five-fold cross-validation, the values were 0.292, 0.495 and 0.476 for the models predicting compressive strength, slump flow diameter and V-funnel time, respectively.

Fig. 6 illustrates the performance of the developed SVM model in the prediction of fresh and hardened properties of SCC mixes. As can be observed, generally the samples from testing datasets aligned well with the 1:1 line, with correlation coefficients of 0.968, 0.911, and 0.949, respectively. In addition, more details on the estimation accuracy of SVM models could be obtained by the statistical parameters given in Tables 3 and 4. For instance, the R^2, *RMSE* and *MAE* values of developed RBF-SVM models for compressive strength were 0.936, 5.311 and 4.000, respectively, while these parameters for initial RBF-SVM models were 0.860, 7.721 and 5.847,

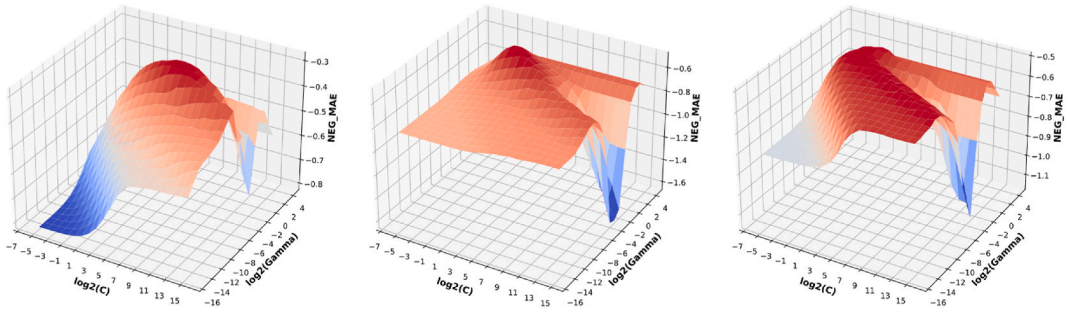

(a) Parameter pairs of Fcu (b) Parameter pairs of SD (c) Parameter pairs of VF

Fig. 5. Negative *MAE* as a function of $log_2(C)$ and $log_2(gamma)$.

Table 4
Values of kernel parameters and statistical results of developed SVM models.

Output variable	RBF parameters selection			Statistical parameters of developed SVM		
	C	*gamma*	*MAE*	R^2	*RMSE*	*MAE*
Fcu	32	0.125	0.292	0.936	5.311	4.000
SD	4	0.125	0.495	0.831	25.153	19.498
VF	32	0.031	0.476	0.901	1.000	0.806

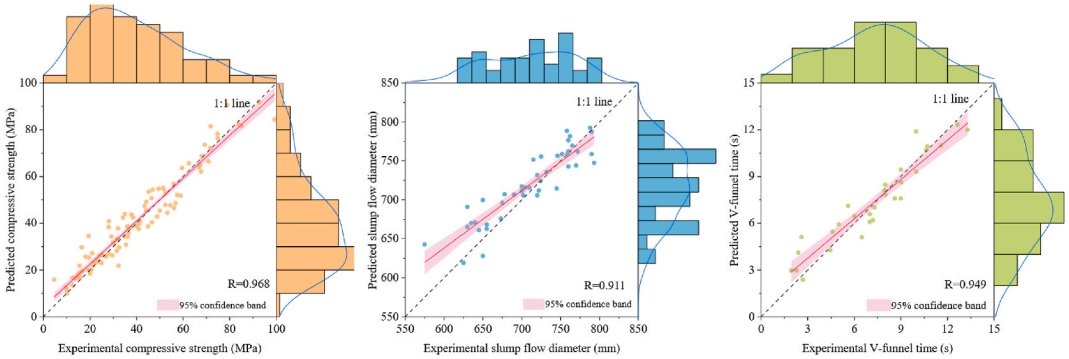

Fig. 6. Correlation between the experimental and predicted values of SCC properties of SVM.

respectively. In this case, the MAE values assessed the performance of the models on the testing datasets. Furthermore, the R^2 values had increased by 8%, 13% and 1% due to the optimization using grid search. Consequently, optimizing the kernel parameters lead to obtaining a more accurate SVM model for predicting the properties of SCC mixes, with a particular emphasis on the improvement in predicting the slump flow diameter.

5.1.2. Prediction of decision tree and random forest models

To improve the performance of regression models, it is of paramount importance to identify the optimal hyperparameter combinations for the decision trees and random forests. This study employed the Scikit-learn Library in Python to accomplish the parameter tuning. During this process, the training dataset was fed into the model, and grid search combined with five-fold cross-validation was utilized to continuously adjust the parameter combination. The objective is to obtain the maximum R^2 value, ultimately leading to the determination of the optimal parameter combinations.

Decision tree and random forest regressors included 11 and 17 parameters, respectively. This study focuses on selecting the primary parameters for each model that have the most significant influence on prediction accuracy. Taking both the processing time and performance of the algorithms into account, this paper provides several suitable values for the selected parameters. The value ranges and optimized values for each parameter of the two models are shown in Table 5. Subsequently, best parameter combinations were employed to construct the new models. The comparison of original models and optimized models are given in Fig. 7, where scores are represented by R^2 values. The results indicate that the grid search has benefits on the prediction performance of both decision tree and random forest models.

Fig. 8 demonstrates the performance of the optimized decision tree and random forest models in predicting fresh and hardened properties of SCC mixes. For the decision tree model, the correlation coefficients of experimental and predicted variables were 0.959, 0.913 and 0.946, respectively. The coefficients in the RF model were 0.977, 0.930 and 0.956, respectively. In general, the random forest models gave more accurate predictions for the testing dataset of the three output properties. By developing random forest models, the correlation coefficient of each output variable increased by 1.9%, 1.9% and 1.2%, respectively.

Table 5
Selection of hyperparameters of decision tree and random forest from the grid search.

Hyperparameters	Range	Tuned values of RF			Tuned values of DT		
		Fcu	SD	VF	Fcu	SD	VF
n_estimators	(100,150,200,300,500)	100	100	100	–	–	–
max_depth	[10,20]	17	15	16	17	15	13
min_impurity_decrease	(0,0.001,0.01,0.1,0.2)	0	0	0	0	0	0
min_samples_leaf	(1,2,5,8,10)	1	1	1	1	1	1
min_samples_split	(2,5,8,10)	2	2	2	2	2	2
random state	[1,1000]	332	83	623	1	6	10

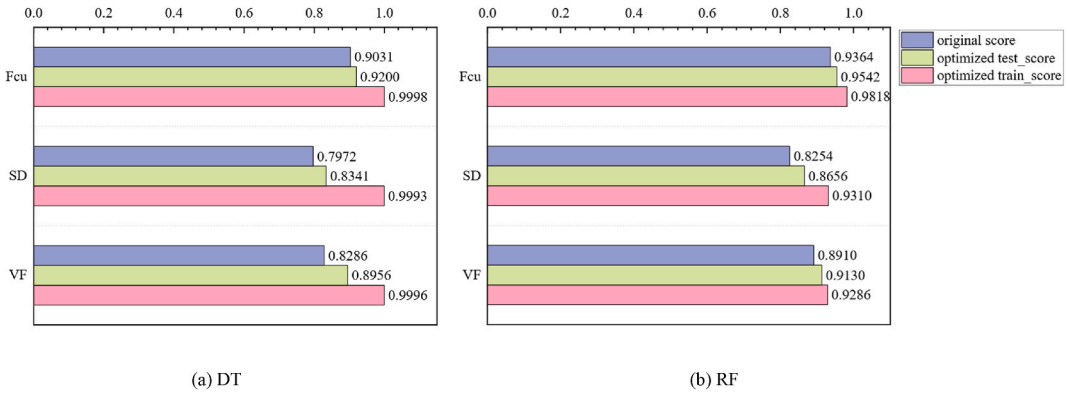

Fig. 7. Accuracy (R^2 values) of optimized models in decision tree and random forest models.

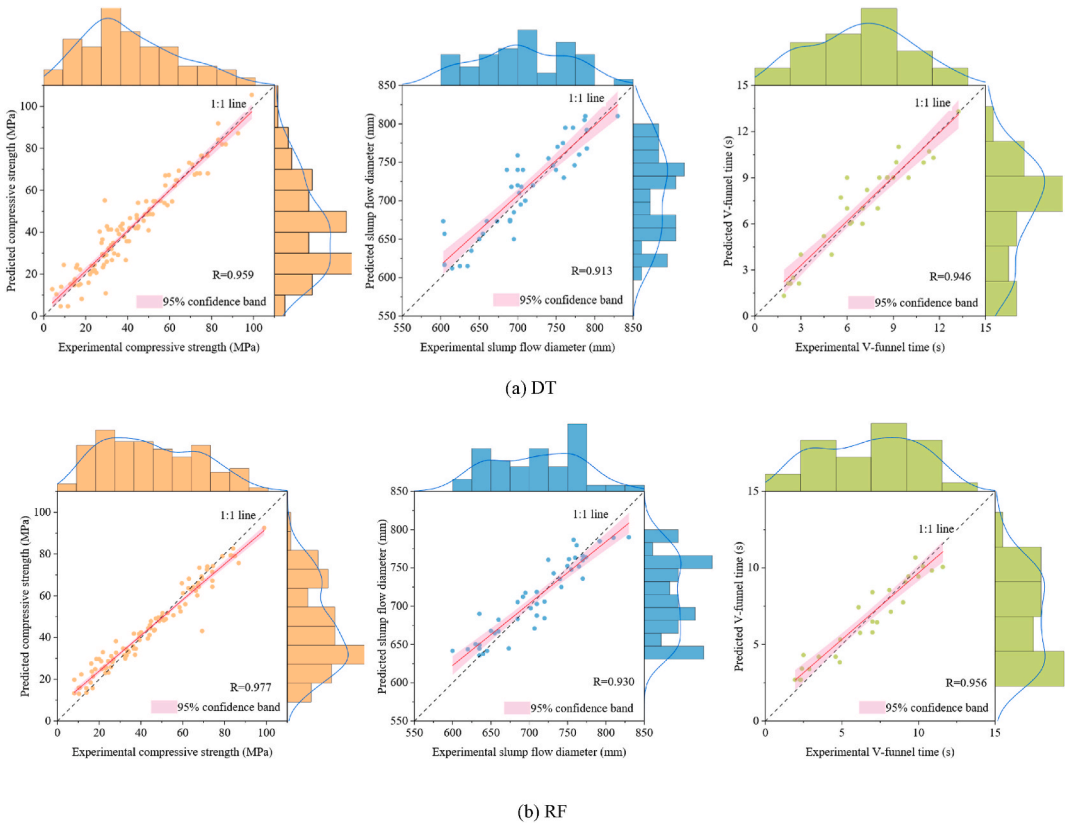

Fig. 8. Correlation between the experimental and predicted values of SCC properties.

5.1.3. Prediction of ANN model

To conduct an ANN model with good applicability, a MATLAB program was developed (R2021a). The networks with one hidden layer were chosen and Levenberg-Marquardt was defined as the training algorithm. All parameters for training ANN models are summarized in Table 6. The maximum training epoch and validation checking epoch were set to be twenty and six iterations, respectively. The calculation stopped when the error is smaller than 10^{-6}. The normalized datasets were split into three groups, with 80% for training and 20% for testing, maintaining the same scale as the testing dataset for previous algorithms. In order to circumvent the issue of overfitting, this study carefully considered the number of neurons present within the hidden layer. A comprehensive exploration of models was conducted, wherein the number of nodes in the hidden layer was systematically varied from 5 to 15. The model's generalization capability and accuracy were assessed through the R^2 and *RMSE* metrics, as derived from the training datasets. The findings, as depicted in Fig. 9, enabled the identification of optimal models, characterized by the highest R^2 values and the lowest *RMSE* s.

Table 6
Parameters selection and performance of ANN models.

	Fcu	SD	VF
Parameters			
Number of input variables	7	6	6
Number of the hidden layer	1		
Number of neurons in the hidden layer	10	10	8
Number of output variables		1	
Training function		Levenberg-Marquardt	
Transfer functions		Sigmoid for hidden layer	
Training epoch		20 iterations	
Training error	10^{-6}		
Measurements			
R^2	0.927	0.694	0.783
RMSE	5.568	35.224	1.675
MAE	4.111	26.633	1.367

The evaluation metrics for the selected models, featuring optimal hidden node numbers, are presented in Table 6. As can be seen, the proposed ANN model for the prediction of compressive strength had the highest accuracy, with R^2 of 0.927, in comparison with the prediction of slump flow and V-funnel time. However, the *RMSE* and *MSE* values in the prediction of slump flow were significantly higher than others. As demonstrated in Fig. 10, there were more scattered data points away from the line of equality between experimental and predicted slump flow results. The correlation coefficients for the output variables were 0.963, 0.833 and 0.885, respectively. In general, the output values predicted by ANN models showed significant correlations with experimental data and the network provided reasonable estimation accuracies.

5.2. Comparison of machine learning models

In this section, a comparative assessment of four machine learning algorithms in terms of predicting SCC properties is presented. The values of R^2, *RMSE* and *MAE* and the dispersion degrees of the predicted result scatters were considered as the reasonable measures to judge the accuracy of the proposed models. In general, the machine learning models were able to predict all output variables in the test datasets with reasonable accuracy.

Table 7 shows a comprehensive comparison between the precision of four machine learning algorithms using the same datasets for each property. It can be clearly noticed that the proposed random forest models exhibited superior performance compared to the other algorithms for each SCC performance index, as evidenced by the R^2 values ranging from 0.8656 to 0.9542. In addition to the decision tree models, the proposed models behaved best in terms of predicting compressive strength, where the maximum R^2 was 0.9199. On the other hand, the slump flow spread diameter was more challenging to predict than the other two properties, as the minimum R^2 was 0.6938 achieved by ANN model. In case of all predicted characteristics, the values of *RMSE* and *MAE* were relative higher in the prediction of the slump flow spread.

To visualize the comparison among the results better, the regression error characteristic (REC) curve was used in estimating the accuracy of all machine learning models [21]. The REC curve presents the relationship between the error tolerance (x-axis) and the percentage of predicted results in the tolerance (y-axis). The curves express the cumulative distribution function of errors. The area over the curve defines the performance of the models, with a smaller area indicating higher accuracy. The REC curve for a perfect model should coincide with the y-axis. Fig. 11 shows the REC curves of all models for the predicting of the compressive strength, slump flow spread diameter and V-funnel time, respectively. The values of area over REC curves and the corresponding area ratios are given in Table 8. Overall, the area ratios of the prediction of compressive strength were on the lower side. Besides, the random forest models consistently achieved the lowest area ratios and therefore, appeared to be the best performing models for modelling SCC properties.

In addition to REC curves, the Taylor diagrams were also employed to compare the accuracy of the three parameters as shown in Fig. 12. The plot measures the respective distance between each model and the reference point labelled as 'Ref'. Decision tree models

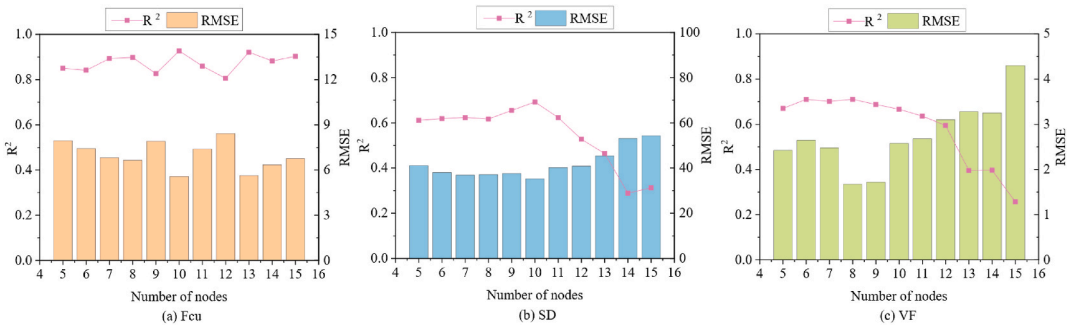

Fig. 9. Accuracy and generalization of models versus the number of hidden layer nodes.

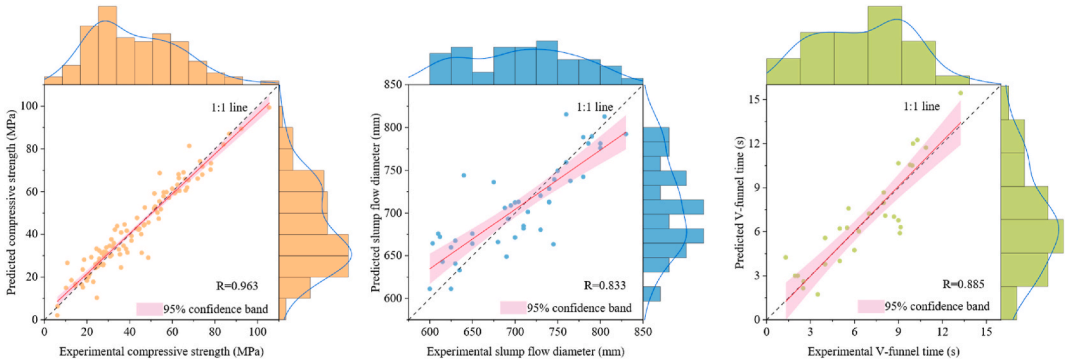

Fig. 10. Correlation between the experimental and predicted values of SCC properties of ANN.

Table 7
Performance of tests metrics (20%) of various machine learning algorithms.

Models	Characteristic	R^2	*RMSE*	*MAE*
SVM	Fcu	0.9363	5.3107	3.9999
	SD	0.8306	25.1535	19.4980
	VF	0.9009	0.9997	0.8061
DT	Fcu	0.9199	6.2417	4.6440
	SD	0.8340	25.5630	19.4031
	VF	0.8956	1.0247	0.8014
RF	Fcu	0.9542	5.3037	3.7623
	SD	0.8656	21.1175	16.8765
	VF	0.9130	0.9154	0.7962
ANN	Fcu	0.9269	5.5678	4.1113
	SD	0.6938	35.2245	26.6335
	VF	0.7830	1.6751	1.3670

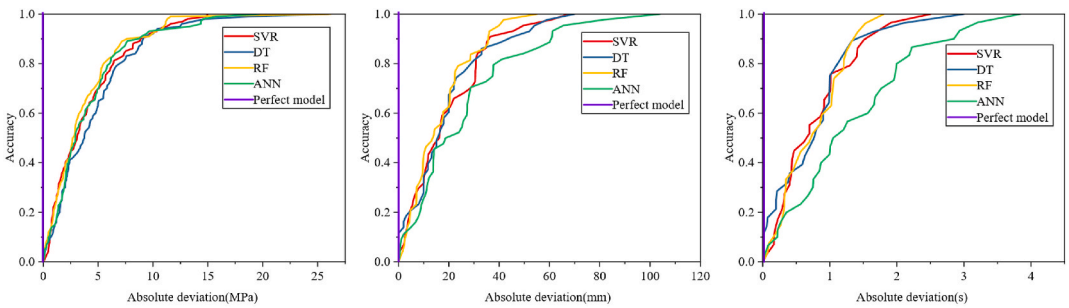

Fig. 11. REC curves of tests metrics (20%) of various machine learning algorithms (a) Fcu, (b) SD, (c) VF.

Table 8
The area over REC curves and area ratios of various machine learning algorithms.

Properties	Absolute area				Area ratio (%)			
	SVM	DT	RF	ANN	SVM	DT	RF	ANN
Fcu	3.926	4.514	**3.631**	4.014	7.851	9.028	**7.263**	8.027
SD	18.729	18.589	**16.236**	25.451	20.810	20.655	**18.040**	28.279
VF	0.763	0.745	**0.739**	1.303	15.258	14.904	**14.772**	26.059

showed the highest standard deviation in all predictions, indicating that the predicted values were more spread out from the mean value compared to the other models. The random forest models, which exhibited lower *RMSE* values and higher correlation coefficient values, were found to be located closer to the true data points. This indicated that the random forest models appeared to be the best performing models for modelling SCC properties, which is fairly consistent with the previous discussion.

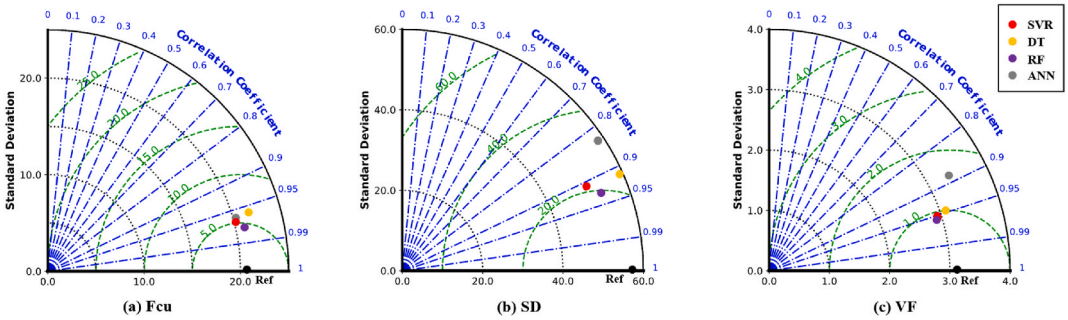

Fig. 12. Taylor diagrams of different machine learning models for SCC prediction.

In summary, from the statistical analysis and the visual interpretation of predictive performance of four machine learning algorithms, the random forest models were proven to demonstrate the highest accuracy among all. This superior performance can be attributed to the ensemble learning characteristic of the random forest. This ensemble approach could enhance performance compared to individual models like the decision tree, helping reduce variance and the risk of overfitting [82]. For instance, the training scores of decision tree for predicting all SCC properties are high, often exceeding 0.999, as shown in Fig. 7. However, despite these high training scores, the accuracy of the decision tree models on the test datasets tends to be nearly 0.03 lower than that of the random forest models. Furthermore, random forest is less sensitive to outliers in the dataset than SVM and ANN, due to the method of aggregating the prediction from multiple trees [83]. Moreover, random forest can effectively capture the nonlinear relationship between the compositions and properties of SCC [84], while SVR and DT may struggle with the complex patterns. Additionally, when compared with SVM and ANN models, random forest models showed great potential due to the visual tree structure, which can be easily understood even by non-experts. Although the ANN models exhibited comparatively inferior performance relative to the other models, they still demonstrated a satisfactory level of accuracy.

The models proposed in this study were compared with others highlighted in the current literature, as illustrated in Fig. 13. For the purposes of this comparison, the correlation coefficient (testing set only) was employed as the benchmark criterion. It is evident that all the models under investigation predict the compressive strength of SCC more accurately than its fresh properties. Notably, the algorithms formulated in our study outperformed the majority of the examined models, excelling particularly in predicting both compressive strength and flowability properties of SCC. Comparing our discussions on the V-funnel time prediction with those presented in Ref. [27], despite the comparatively lower R^2 value observed on the test set, the smaller RMSE ($0.915 < 1.11$) suggests a heightened precision in predictions. Conversely, on the overall dataset, a higher R^2 value ($0.926 > 0.87$) exhibited in the proposed RF model, indicating a superior capacity for explicating variance in the entirety of the data and adeptly accommodating diverse subsets of data. Nonetheless, considering that no model can flawlessly predict SCC properties, there remains potential for further enhancement on the dataset collection and algorithmic approaches.

5.3. *Feature importance of influencing variables*

After conducting a comparison of the predictive performance of all algorithms, the random forest models with optimal hyperparameters were obtained. In conjunction with the SCC characteristics, six features were used for predicting fresh properties, and seven features were employed for predicting compressive strength in the random forest models. Figs. 14 and 15 display the importance of each input variable for the regression models based on the method of Shapley Additive explanation (SHAP) analysis. As a game theory-based approach, in SHAP, the output model is structured as a linear combination of the input variables, determining the contributions of each input variable to every prediction [85].

In Fig. 14, it is revealed that curing age, the content of cement and W/B ratio are the most sensitive factors dominating the compressive strength of SCC mixes, with the mean absolute SHAP value of 9.94, 8.35 and 3.14, respectively. This result is in agreement with the findings of previous studies [32,86,87]. In contrast, the SHAP value of fly ash is 1.04, indicating that the influence of fly ash is relatively less significant. This is because, relatively low chemical activity and hydration rate of fly ash make it less effective than cement in enhancing the early strength of concrete [88]. Similarly, the dosage of SP contributes less to SCC strength, with the SHAP value of 1.05. Conversely, it has the highest influence on predicting the fresh properties of SCC, as shown in Fig. 15. This suggests that the impact of SP on enhancing the workability of concrete is greater than its direct contribution to strength [89].

The SHAP summary plot is also shown in Fig. 14, with the x-axis representing the weight of influence, and the colour of scatter points indicating the impact degree of input variables on the predicted properties [87]. Therefore, a wider regional distribution signifies a greater influence of this variable. It can be observed that the compressive strength of SCC significantly increases with the progression of curing age, higher cement content, and more aggregates. However, a higher water to binder ratio results in a negative SHAP value, indicating a lower compressive strength of SCC. This finding is consistent with published literatures [90–92]. Additionally, the impact of fly ash is opposite to that of cement; an increase in fly ash content decreases SCC compressive strength, as observed in existing experimental investigations [93–95]. Besides, the influence of SP dosage is not as pronounced.

Fig. 15 illustrates the feature importance of six input parameters in predicting SCC fresh properties, as evaluated by mean absolute SHAP values. Following the most influential parameter, SP, water to binder ratio exhibits a strong impact on both slump flow diameter

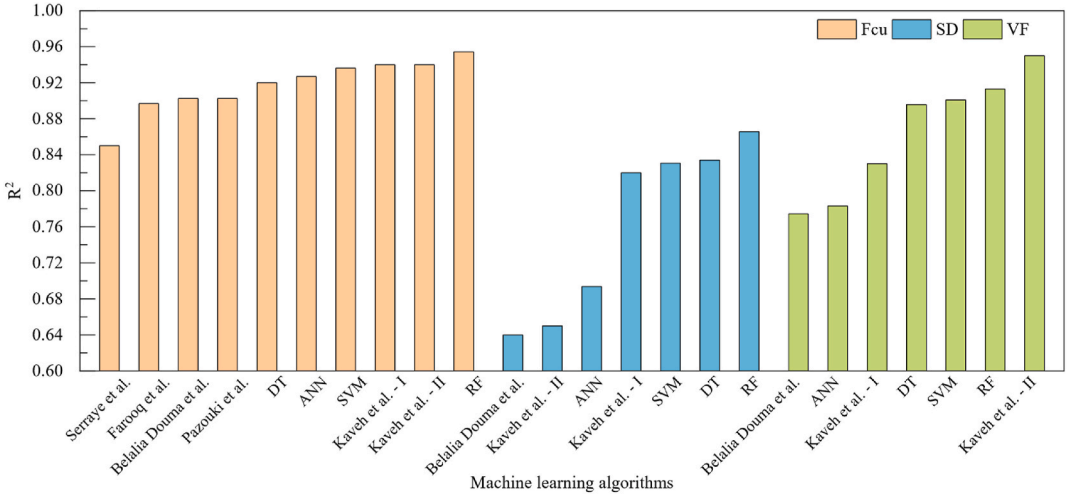

Fig. 13. Comparative analysis of proposed models with existing literature (data from Refs. [26,27,32–34]).

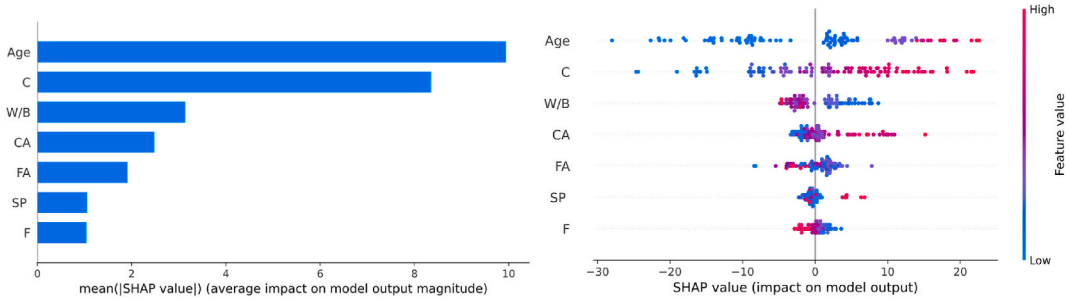

Fig. 14. Feature importance and SHAP summary plot using RF models for predicting Fcu.

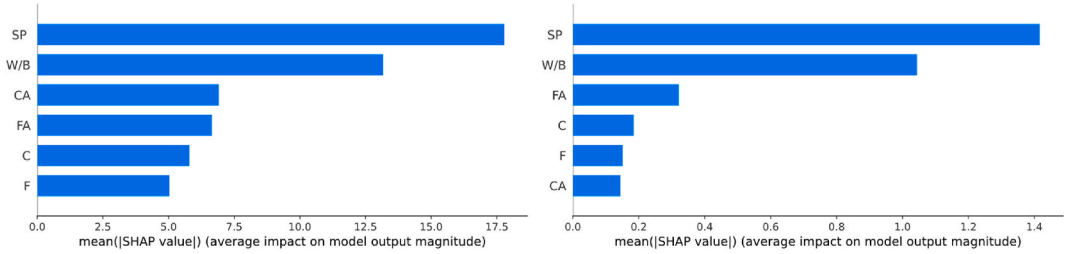

Fig. 15. Feature importance plot using RF models for predicting SD and VF.

and V-funnel time. The significant effect can be observed in existing studies [96–99]. As a main ingredient in SCC, the aggregate content is demonstrated to have considerable effect on the slump flow diameter, as evident in published studies [100]. Compared to other main factors, the content of cement and fly ash has less impact on fresh properties. The flow behaviour of SCC is the result of SP-cement interaction and can be modified by adding cementitious materials such as fly ash. Fly ash promotes the adsorption of SP on cement particles, which depends on the concentration of C3A cement phase and the amount of gypsum in the system [101]. Although both cement and fly ash contribute to the enhancement of microstructure and workability of SCC, their effects in the fresh state are not as pronounced as those of water and chemical additives. It is worth noting that the feature importance analysed in this study are based on the specific dataset used. Thus, the results could be more representative with the expansion of dataset and the inclusion of more variables.

5.4. Potential applications of the proposed data driven framework

The design codes of SCC mixes typically rely on the conventional strength-based mix design methodologies used for normal vibrated concrete [102]. Studies in the past have also suggested reliable SCC mix design tactics that consider both strength and plastic

viscosity [103]. However, the designed characteristics of SCC mixes might be subjected to several constraints because of the additional restrictions on the mixture contents, such as maximum value of W/B ratio and the aggregate contents. Furthermore, the synergistic effect of fly ash and other supplementary materials significantly impacts the properties of SCC, posing a great challenge to the conventional proportioning approach. In response to evolving design prerequisites, there has been a growing demand for a precise and sustainable SCC design and validation framework in the construction industry. Consequently, this section proposes the development of a data driven machine learning framework.

It has been proven in the previous discussion that the optimized machine learning models can accurately predict both fresh and hardened properties of SCC containing fly ash. These models could serve as a pre-experimental validation tool to ensure workload optimization, thus providing robust experimental support. Moreover, the efficacy of this framework can be further enhanced with other SCC proportioning methods by dynamically modulating the dosage of each ingredient in line with predictive outcomes.

The execution of this framework, along with its further development, is depicted in Fig. 16. Initially, the target properties of SCC with fly ash are determined, followed by the calculation of the preliminary proportions based on strength-based mix design methods. These mix proportions are then input into the finely tuned machine learning models to predict SCC properties. By verifying and contrasting with the initial mix design, the dosage of each ingredient is adjusted to a suitable range, resulting in an optimized mix design. To further develop the data driven framework, it is recommended to incorporate larger datasets and more specific variables for model modification and broadening the applicability. Moreover, by considering the structure related parameters and the output from the proposed machine learning models, a more complex framework for structural design and identification could be developed.

5.5. *Limitations of this research*

The discussion on the development and comparative analysis of various predictive models has been carried out, demonstrating the effectiveness of the Random Forest (RF) model in predicting the properties of SCC. While these findings are significant, it is important to acknowledge certain limitations present within this study. All machine learning models were developed and optimized based on comprehensive datasets derived from a significant portion of existing literature on SCC with fly ash. However, the overall size of datasets remains relatively limited. This constraint may affect the generalizability of the models across different SCC mixes. Additionally, while this study considers several critical factors affecting SCC properties, there remains room to include additional variables that might further influence the behaviour of SCC. A more detailed categorization of input variables, based on the characteristics of materials, was not fully explored in current analysis. For instance, factors such as the strength grade of cement, the size of aggregates, and the specific chemical composition of supplementary materials were not thoroughly classified. This limitation could potentially impact the accuracy of developed models. To achieve a balance between the breadth of datasets and the practical constraints, further research involving more experiments could be conducted, ultimately enhancing the robustness of the findings. Furthermore, this study employed a limited selection of four machine learning algorithms. Although these models were proven effectiveness in similar applications, the exclusion of other algorithms may limit the scope of the finding.

6. Conclusion

In this study, four machine learning algorithms, including SVM, decision tree, random forest and ANN were employed to predict both fresh and hardened properties of SCC mixes with fly ash. All models demonstrated the potential to predict these properties with reasonable accuracy. The specific findings of this study are outlined below:

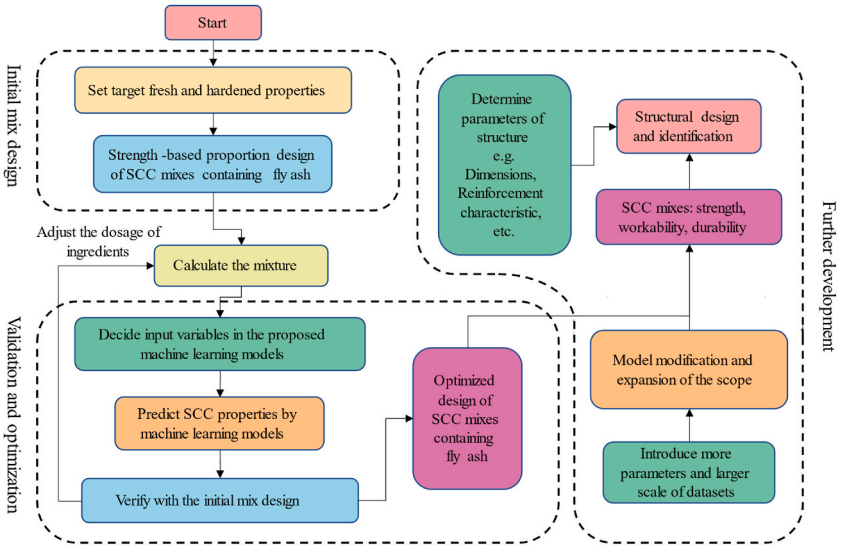

Fig. 16. The application framework of the proposed data driven models and further development.

- Various hyperparameter optimization strategies are examined in detail, with the efficacy of various algorithms subjected to comparative evaluation. These include the choice of kernel functions and grid search techniques in SVM modelling, the determination of key parameters in decision tree and random forest modelling, and the selection process for hidden nodes in ANN modelling.
- The random forest models exhibited the highest accuracy in predicting all SCC properties, as indicated by the high R^2 values of 0.9542, 0.8656 and 0.9130 for compressive strength, slump flow diameter and V-funnel time, respectively. Meanwhile, decision tree, SVM and ANN models also showed promising results.
- The content of cement, curing age, and W/B ratio were found to be the main factors influencing the compressive strength of SCC mixes, which is consistent with previous findings.
- The feature importance analysis indicated that the content of superplasticizers, W/B ratio, and aggregate were the most influential factors on the fresh properties of SCC mixes.
- The REC curves and Taylor diagrams were utilized to compare the performance of all machine learning algorithms used. The random forest models consistently showed the lowest area ratios and smallest distance to the observation point in Taylor diagrams, indicating the highest level of accuracy among the four models.
- The models proposed in this study were compared with others highlighted in the current literature. The algorithms formulated in our study outperformed the majority of the examined models.
- The proposed machine learning models, particularly the random forest models, can provide valuable insights for designing and optimizing SCC mixes containing fly ash, which can ultimately lead to more sustainable construction practices.
- A framework of the proposed data driven approach has been constructed, showcasing significant promise in its practical application. The accuracy of this newly-established structure has been evaluated, focusing on its ability and accuracy in predicting the fresh and hardened properties of SCC.

While the use of three extensive and reliable datasets contributed to accurate predictions of SCC properties containing fly ash, there is potential for further model improvement through the inclusion of additional variables and larger datasets. More efficient hybrid machine learning algorithms can be developed to accelerate the process of parameter tuning and selection. In addition, by leveraging the inherent adaptive learning capabilities of reinforcement learning techniques, the accuracy and efficiency of models are expected to be further enhanced in the application of SCC properties. Meanwhile, the development of models to predict other properties of SCC and soundness of produced structures are recommended for future research.

CRediT authorship contribution statement

Tianyi Cui: Conceptualization, Methodology, Writing – original draft. **Sivakumar Kulasegaram:** Project administration, Supervision, Writing – review & editing. **Haijiang Li:** Methodology, Supervision, Writing – review & editing.

Declaration of competing interest

The authors declare that they have no known competing financial interests or personal relationships that could have appeared to influence the work reported in this paper

Data availability

Data will be made available on request.

Acknowledgment

This work is supported by the China scholarship Council under Grant CSC 202008500151. The author would like to thank them for their support.

Appendix A. Supplementary data

Supplementary data to this article can be found online at https://doi.org/10.1016/j.jobe.2024.108960.

References

[1] H. Okamura, K. Ozawa, Self-compacting high performance concrete, Struct. Eng. Int.: J. Int. Assoc. Bridge Struct. Eng. (IABSE) 6 (1996) 269–270, https://doi.org/10.2749/101686696780496292.
[2] S. Girish, R.V. Ranganath, J. Vengala, Influence of powder and paste on flow properties of SCC, Construct. Build. Mater. 24 (2010) 2481–2488, https://doi.org/10.1016/j.conbuildmat.2010.06.008.
[3] R. Choudhary, R. Gupta, R. Nagar, Impact on fresh, mechanical, and microstructural properties of high strength self-compacting concrete by marble cutting slurry waste, fly ash, and silica fume, Construct. Build. Mater. 239 (2020) 117888, https://doi.org/10.1016/j.conbuildmat.2019.117888.
[4] F. Van Der Vurst, S. Grünewald, D. Feys, K. Lesage, L. Vandewalle, J. Vantomme, G. De Schutter, Effect of the mix design on the robustness of fresh self-compacting concrete, Cem. Concr. Compos. 82 (2017) 190–201, https://doi.org/10.1016/J.CEMCONCOMP.2017.06.005.

[5] B. Felekoğlu, S. Türkel, B. Baradan, Effect of water/cement ratio on the fresh and hardened properties of self-compacting concrete, Build. Environ. 42 (2007) 1795–1802, https://doi.org/10.1016/j.buildenv.2006.01.012.

[6] W.T. Lin, Effects of sand/aggregate ratio on strength, durability, and microstructure of self-compacting concrete, Construct. Build. Mater. 242 (2020) 118046, https://doi.org/10.1016/J.CONBUILDMAT.2020.118046.

[7] P. Niewiadomski, J. Hoła, Failure process of compressed self-compacting concrete modified with nanoparticles assessed by acoustic emission method, Autom. ConStruct. 112 (2020), https://doi.org/10.1016/j.autcon.2020.103111.

[8] G. Long, Y. Gao, Y. Xie, Designing more sustainable and greener self-compacting concrete, Construct. Build. Mater. 84 (2015) 301–306, https://doi.org/10.1016/j.conbuildmat.2015.02.072.

[9] Y. Gamil, J. Nilimaa, T. Najeh, A. Cwirzen, Formwork pressure prediction in cast-in-place self-compacting concrete using deep learning, Autom. ConStruct. 151 (2023), https://doi.org/10.1016/j.autcon.2023.104869.

[10] K.A. Melo, A.M.P. Carneiro, Effect of Metakaolin's finesses and content in self-consolidating concrete, Construct. Build. Mater. 24 (2010) 1529–1535, https://doi.org/10.1016/J.CONBUILDMAT.2010.02.002.

[11] S. Dadsetan, J. Bai, Mechanical and microstructural properties of self-compacting concrete blended with metakaolin, ground granulated blast-furnace slag and fly ash, Construct. Build. Mater. 146 (2017) 658–667, https://doi.org/10.1016/J.CONBUILDMAT.2017.04.158.

[12] G. Ling, Z. Shui, T. Sun, X. Gao, Y. Wang, Y. Sun, G. Wang, Z. Li, Rheological behavior and microstructure characteristics of SCC incorporating metakaolin and silica fume, Materials 11 (2018), https://doi.org/10.3390/ma11122576.

[13] N. Makul, Combined use of untreated-waste rice husk ash and foundry sand waste in high-performance self-consolidating concrete, Results in Materials 1 (2019) 100014, https://doi.org/10.1016/J.RINMA.2019.100014.

[14] R.H. Faraj, A.F.H. Sherwani, L.H. Jafer, D.F. Ibrahim, Rheological behavior and fresh properties of self-compacting high strength concrete containing recycled PP particles with fly ash and silica fume blended, J. Build. Eng. 34 (2021) 101667, https://doi.org/10.1016/j.jobe.2020.101667.

[15] Y.T.H. Cu, M.V. Tran, C.H. Ho, P.H. Nguyen, Relationship between workability and rheological parameters of self-compacting concrete used for vertical pump up to supertall buildings, J. Build. Eng. 32 (2020) 101786, https://doi.org/10.1016/j.jobe.2020.101786.

[16] L.D.A. Schwartzentruber, R. Le Roy, J. Cordin, Rheological behaviour of fresh cement pastes formulated from a Self Compacting Concrete (SCC), Cement Concr. Res. 36 (2006) 1203–1213, https://doi.org/10.1016/j.cemconres.2004.10.036.

[17] M.Y. Cheng, J.S. Chou, A.F.V. Roy, Y.W. Wu, High-performance concrete compressive strength prediction using time-weighted evolutionary fuzzy support vector machines inference model, Autom. ConStruct. 28 (2012) 106–115, https://doi.org/10.1016/j.autcon.2012.07.004.

[18] B.A. Young, A. Hall, L. Pilon, P. Gupta, G. Sant, Can the compressive strength of concrete be estimated from knowledge of the mixture proportions?: new insights from statistical analysis and machine learning methods, Cement Concr. Res. 115 (2019) 379–388, https://doi.org/10.1016/J.CEMCONRES.2018.09.006.

[19] J. Sun, J. Zhang, Y. Gu, Y. Huang, Y. Sun, G. Ma, Prediction of permeability and unconfined compressive strength of pervious concrete using evolved support vector regression, Construct. Build. Mater. 207 (2019) 440–449, https://doi.org/10.1016/j.conbuildmat.2019.02.117.

[20] A. Behnood, K.P. Verian, M. Modiri Gharehveran, Evaluation of the splitting tensile strength in plain and steel fiber-reinforced concrete based on the compressive strength, Construct. Build. Mater. 98 (2015) 519–529, https://doi.org/10.1016/j.conbuildmat.2015.08.124.

[21] P.G. Asteris, A.D. Skentou, A. Bardhan, P. Samui, K. Pilakoutas, Predicting concrete compressive strength using hybrid ensembling of surrogate machine learning models, Cement Concr. Res. 145 (2021) 106449, https://doi.org/10.1016/J.CEMCONRES.2021.106449.

[22] A. Nafees, M.N. Amin, K. Khan, K. Nazir, M. Ali, M.F. Javed, F. Aslam, M.A. Musarat, N.I. Vatin, Modeling of mechanical properties of silica fume-based green concrete using machine learning techniques, Polymers 14 (2022), https://doi.org/10.3390/polym14010030.

[23] Yogesh Aggarwal, Paratibha Aggarwal, R. Siddique, P. Aggarwal, Y. Aggarwal, Prediction of compressive strength of self-compacting concrete containing bottom ash using artificial neural networks, I. J. Math. Comput. Sci. 5 (2011) 762–767, https://doi.org/10.1016/j.advengsoft.2011.05.016.

[24] P.G. Asteris, K.G. Kolovos, M.G. Douvika, K. Roinos, Prediction of self-compacting concrete strength using artificial neural networks, Eur. J. Environ. and Civil Eng. 20 (2016) s102, https://doi.org/10.1080/19648189.2016.1246693. –s122.

[25] E.M. Golafshani, A. Ashour, Prediction of self-compacting concrete elastic modulus using two symbolic regression techniques, Autom. ConStruct. 64 (2016) 7–19, https://doi.org/10.1016/J.AUTCON.2015.12.026.

[26] O. Belalia Douma, B. Boukhatem, M. Ghrici, A. Tagnit-Hamou, Prediction of properties of self-compacting concrete containing fly ash using artificial neural network, Neural Comput. Appl. 28 (2017) 707–718, https://doi.org/10.1007/s00521-016-2368-7.

[27] A. Kaveh, T. Bakhshpoori, S.M. Hamze-Ziabari, M5' and mars based prediction models for properties of selfcompacting concrete containing fly ash, Period. Polytech. Civ. Eng. 62 (2018) 281–294, https://doi.org/10.3311/PPci.10799.

[28] P.G. Asteris, K.G. Kolovos, Self-compacting concrete strength prediction using surrogate models, Neural Comput. Appl. 31 (2019) 409–424, https://doi.org/10.1007/s00521-017-3007-7.

[29] P. Saha, P. Debnath, P. Thomas, Prediction of fresh and hardened properties of self-compacting concrete using support vector regression approach, Neural Comput. Appl. 32 (2020) 7995–8010, https://doi.org/10.1007/s00521-019-04267-w.

[30] M. Azimi-Pour, H. Eskandari-Naddaf, A. Pakzad, Linear and non-linear SVM prediction for fresh properties and compressive strength of high volume fly ash self-compacting concrete, Construct. Build. Mater. 230 (2020), https://doi.org/10.1016/j.conbuildmat.2019.117021.

[31] S. Kumar, B. Rai, R. Biswas, P. Samui, D. Kim, Prediction of rapid chloride permeability of self-compacting concrete using multivariate adaptive regression spline and minimax probability machine regression, J. Build. Eng. 32 (2020), https://doi.org/10.1016/j.jobe.2020.101490.

[32] F. Farooq, S. Czarnecki, P. Niewiadomski, F. Aslam, H. Alabduljabbar, K.A. Ostrowski, K. Sliwa-Wieczorek, T. Nowobilski, S. Malazdrewicz, A comparative study for the prediction of the compressive strength of self-compacting concrete modified with fly ash, Materials (2021), https://doi.org/10.3390/ma14174934.

[33] M. Serraye, S. Kenai, B. Boukhatem, Prediction of compressive strength of self-compacting concrete (SCC) with silica fume using neural networks models, Civil Engineering Journal (Iran) 7 (2021) 118–139, https://doi.org/10.28991/cej-2021-03091642.

[34] G. Pazouki, E.M. Golafshani, A. Behnood, Predicting the Compressive Strength of Self-Compacting Concrete Containing Class F Fly Ash Using Metaheuristic Radial Basis Function Neural Network, Structural Concrete, 2021, https://doi.org/10.1002/suco.202000047.

[35] E.A. Yousef, B.A. Mouhcine, Z. Mounir, H.A. Adil, Prediction of compressive strength of self-compacting concrete using four machine learning technics, Mater. Today Proc. (2022), https://doi.org/10.1016/j.matpr.2022.02.487.

[36] M. Ben Aicha, Y. Al Asri, M. Zaher, A.H. Alaoui, Y. Burtschell, Prediction of rheological behavior of self-compacting concrete by multi-variable regression and artificial neural networks, Powder Technol. 401 (2022) 117345, https://doi.org/10.1016/j.powtec.2022.117345.

[37] J. de-Prado-Gil, C. Palencia, N. Silva-Monteiro, R. Martínez-García, To predict the compressive strength of self compacting concrete with recycled aggregates utilizing ensemble machine learning models, Case Stud. Constr. Mater. 16 (2022) e01046, https://doi.org/10.1016/j.cscm.2022.e01046.

[38] N. Abunassar, M. Alas, S.I.A. Ali, Prediction of compressive strength in self-compacting concrete containing fly ash and silica fume using ANN and SVM, Arabian J. Sci. Eng. (2022), https://doi.org/10.1007/s13369-022-07359-3.

[39] R.H. Faraj, A.A. Mohammed, K.M. Omer, H.U. Ahmed, Soft computing techniques to predict the compressive strength of green self-compacting concrete incorporating recycled plastic aggregates and industrial waste ashes, Clean Technol. Environ. Policy 24 (2022) 2253–2281, https://doi.org/10.1007/s10098-022-02318-w.

[40] V. Vapnik, The Nature of Statistical Learning Theory, Springer science \& business media, 1999.

[41] C. Cortes, V. Vapnik, L. Saitta, Support-Vector Networks Editor, Kluwer Academic Publishers, 1995.

[42] H. Drucker, C.J.C. Burges, L. Kaufman, A. Smola, V. Vapnik, Support vector regression machines, in: Advances in Neural Information Processing Systems, vol. 9, NIPS 1996, 1996, pp. 155–161.

[43] V.D.A. Sánchez, Advanced support vector machines and kernel methods, Neurocomputing 55 (2003) 5–20, https://doi.org/10.1016/S0925-2312(03)00373-4.

[44] C.-W. Hsu, C.-C. Chang, C.-J. Lin, A Practical Guide to Support Vector Classification, 2003, pp. 1–16.

[45] G.K.F. Tso, K.K.W. Yau, Predicting electricity energy consumption: a comparison of regression analysis, decision tree and neural networks, Energy 32 (2007) 1761–1768, https://doi.org/10.1016/j.energy.2006.11.010.
[46] M.H. Beale, M.T. Hagan, H.B. Demuth, Neural Network Toolbox™ 7 User's Guide, 2010, https://doi.org/10.1016/j.fuel.2020.118589.
[47] A.W.C. Oreta, K. Kawashima, Neural network modeling of confined compressive strength and strain of circular concrete columns, J. Struct. Eng. 129 (2003) 554–561, https://doi.org/10.1061/(asce)0733-9445, 2003)129:4(554.
[48] R. Bro, K. Kjeldahl, A.K. Smilde, H.A.L. Kiers, Cross-validation of component models: a critical look at current methods, Anal. Bioanal. Chem. 390 (2008) 1241–1251, https://doi.org/10.1007/s00216-007-1790-1.
[49] R. Kohavi, A Study of Cross-Validation and Bootstrap for Accuracy Estimation and Model Selection, 1995. http://robotics.stanford.edu/~ronnyk.
[50] J.M. Khatib, Performance of self-compacting concrete containing fly ash, Construct. Build. Mater. 22 (2008) 1963, https://doi.org/10.1016/J.CONBUILDMAT.2007.07.011. –1971.
[51] B. Sukumar, K. Nagamani, R. Srinivasa Raghavan, Evaluation of strength at early ages of self-compacting concrete with high volume fly ash, Construct. Build. Mater. 22 (2008) 1394–1401, https://doi.org/10.1016/J.CONBUILDMAT.2007.04.005.
[52] M. Sonebi, A. Cevik, Prediction of fresh and hardened properties of self-consolidating concrete using neurofuzzy approach, J. Mater. Civ. Eng. 21 (2009) 672–679, https://doi.org/10.1061/(asce)0899-1561, 2009)21:11(672.
[53] E. Güneyisi, Fresh properties of self-compacting rubberized concrete incorporated with fly ash, Materials and Structures/Materiaux et Constructions 43 (2010) 1037–1048, https://doi.org/10.1617/s11527-009-9564-1.
[54] M. Liu, Self-compacting concrete with different levels of pulverized fuel ash, Construct. Build. Mater. 24 (2010) 1245–1252, https://doi.org/10.1016/J.CONBUILDMAT.2009.12.012.
[55] M. Şahmaran, M. Lachemi, T.K. Erdem, H.E. Yücel, Use of spent foundry sand and fly ash for the development of green self-consolidating concrete, Materials and Structures/Materiaux et Constructions 44 (2011) 1193–1204, https://doi.org/10.1617/s11527-010-9692-7.
[56] R. Siddique, Properties of self-compacting concrete containing class F fly ash, Mater. Des. 32 (2011) 1501–1507, https://doi.org/10.1016/J.MATDES.2010.08.043.
[57] M. Jalal, E. Mansouri, Effects of fly ash and cement content on rheological, mechanical, and transport properties of high-performance self-compacting concrete, Sci. Eng. Compos. Mater. 19 (2012) 393–405, https://doi.org/10.1515/secm-2012-0052.
[58] M. Uysal, K. Yilmaz, M. Ipek, The effect of mineral admixtures on mechanical properties, chloride ion permeability and impermeability of self-compacting concrete, Construct. Build. Mater. 27 (2012) 263–270, https://doi.org/10.1016/J.CONBUILDMAT.2011.07.049.
[59] J. Cuenca, J. Rodríguez, M. Martín-Morales, Z. Sánchez-Roldán, M. Zamorano, Effects of olive residue biomass fly ash as filler in self-compacting concrete, Construct. Build. Mater. 40 (2013) 702–709, https://doi.org/10.1016/J.CONBUILDMAT.2012.09.101.
[60] P. Ramanathan, I. Baskar, P. Muthupriya, R. Venkatasubramani, Performance of self-compacting concrete containing different mineral admixtures, KSCE J. Civ. Eng. 17 (2013) 465–472, https://doi.org/10.1007/s12205-013-1882-8.
[61] H. Siad, S. Kamali-Bernard, H.A. Mesbah, G. Escadeillas, M. Mouli, H. Khelafi, Characterization of the degradation of self-compacting concretes in sodium sulfate environment: influence of different mineral admixtures, Construct. Build. Mater. 47 (2013) 1188–1200, https://doi.org/10.1016/J.CONBUILDMAT.2013.05.086.
[62] M.C.S. Nepomuceno, L.A. Pereira-De-Oliveira, S.M.R. Lopes, Methodology for the mix design of self-compacting concrete using different mineral additions in binary blends of powders, Construct. Build. Mater. 64 (2014) 82–94, https://doi.org/10.1016/j.conbuildmat.2014.04.021.
[63] T. Ponikiewski, J. Gołaszewski, The effect of high-calcium fly ash on selected properties of self-compacting concrete, Arch. Civ. Mech. Eng. 14 (2014) 455–465, https://doi.org/10.1016/j.acme.2013.10.014.
[64] E. Güneyisi, M. Gesoglu, A. Al-Goody, S. Ipek, Fresh and rheological behavior of nano-silica and fly ash blended self-compacting concrete, Construct. Build. Mater. 95 (2015) 29–44, https://doi.org/10.1016/j.conbuildmat.2015.07.142.
[65] H. Zhao, W. Sun, X. Wu, B. Gao, The properties of the self-compacting concrete with fly ash and ground granulated blast furnace slag mineral admixtures, J. Clean. Prod. 95 (2015) 66–74, https://doi.org/10.1016/j.jclepro.2015.02.050.
[66] R. Bani Ardalan, A. Joshaghani, R.D. Hooton, Workability retention and compressive strength of self-compacting concrete incorporating pumice powder and silica fume, Construct. Build. Mater. 134 (2017) 116–122, https://doi.org/10.1016/J.CONBUILDMAT.2016.12.090.
[67] A.R. Esquinas, E.F. Ledesma, R. Otero, J.R. Jiménez, J.M. Fernández, Mechanical behaviour of self-compacting concrete made with non-conforming fly ash from coal-fired power plants, Construct. Build. Mater. 182 (2018) 385–398, https://doi.org/10.1016/J.CONBUILDMAT.2018.06.094.
[68] P.R. de Matos, M. Foiato, L.R. Prudêncio, Ecological, fresh state and long-term mechanical properties of high-volume fly ash high-performance self-compacting concrete, Construct. Build. Mater. 203 (2019) 282–293, https://doi.org/10.1016/j.conbuildmat.2019.01.074.
[69] M.A.S. Anjos, A. Camões, P. Campos, G.A. Azeredo, R.L.S. Ferreira, Effect of high volume fly ash and metakaolin with and without hydrated lime on the properties of self-compacting concrete, J. Build. Eng. 27 (2020) 100985, https://doi.org/10.1016/J.JOBE.2019.100985.
[70] Z. Guo, T. Jiang, J. Zhang, X. Kong, C. Chen, D.E. Lehman, Mechanical and durability properties of sustainable self-compacting concrete with recycled concrete aggregate and fly ash , slag and silica fume, Construct. Build. Mater. 231 (2020) 117115, https://doi.org/10.1016/j.conbuildmat.2019.117115.
[71] T.Z.H. Ting, M.E. Rahman, H.H. Lau, Sustainable lightweight self-compacting concrete using oil palm shell and fly ash, Construct. Build. Mater. 264 (2020) 120590, https://doi.org/10.1016/J.CONBUILDMAT.2020.120590.
[72] A. Sambangi, E. Arunakanthi, Fresh and mechanical properties of SCC with fly ash and copper slag as mineral admixtures, Mater. Today Proc. 45 (2021) 6687–6693, https://doi.org/10.1016/J.MATPR.2020.12.144.
[73] H. Zhao, W. Sun, X. Wu, B. Gao, Sustainable self-compacting concrete containing high-amount industrial by-product fly ash as supplementary cementitious materials, Environ. Sci. Pollut. Control Ser. 29 (2022) 3616–3628, https://doi.org/10.1007/s11356-021-15883-2/. Published.
[74] S. Kumar, P. Murthi, P. Awoyera, R. Gobinath, S. Kumar, Impact resistance and strength development of fly ash based self-compacting concrete, Silicon 14 (2022) 481–492, https://doi.org/10.1007/s12633-020-00842-2/. Published.
[75] A. Jain, R. Gupta, S. Chaudhary, Sustainable development of self-compacting concrete by using granite waste and fly ash, Construct. Build. Mater. 262 (2020) 120516, https://doi.org/10.1016/J.CONBUILDMAT.2020.120516.
[76] B.N. Kumar, P.P. Kumar, Prediction on flexural strength of high strength hybrid fiber self compacting concrete by using artificial intelligence, Journal of Artificial Intelligence and Capsule Networks 4 (2022) 1–16, https://doi.org/10.36548/jaicn.2022.1.001.
[77] J. Adler, I. Parmryd, Quantifying colocalization by correlation: the pearson correlation coefficient is superior to the Mander's overlap coefficient, Cytometry 77 (2010) 733–742, https://doi.org/10.1002/cyto.a.20896.
[78] M. Ahsan, M. Mahmud, P. Saha, K. Gupta, Z. Siddique, Effect of data scaling methods on machine learning algorithms and model performance, Technologies 9 (2021) 52, https://doi.org/10.3390/technologies9030052.
[79] M. Sonebi, A. Cevik, S. Grünewald, J. Walraven, Modelling the fresh properties of self-compacting concrete using support vector machine approach, Construct. Build. Mater. 106 (2016) 55–64, https://doi.org/10.1016/j.conbuildmat.2015.12.035.
[80] S. Nakagawa, H. Schielzeth, A general and simple method for obtaining R2 from generalized linear mixed-effects models, Methods Ecol. Evol. 4 (2013) 133–142, https://doi.org/10.1111/j.2041-210x.2012.00261.x.
[81] V. Cherkassky, Y. Ma, Practical selection of SVM parameters and noise estimation for SVM regression, Neural Network. 17 (2004) 113–126, https://doi.org/10.1016/S0893-6080(03)00169-2.
[82] M.C. Kang, D.Y. Yoo, R. Gupta, Machine learning-based prediction for compressive and flexural strengths of steel fiber-reinforced concrete, Construct. Build. Mater. 266 (2021), https://doi.org/10.1016/j.conbuildmat.2020.121117.
[83] B. Dev, M.A. Rahman, M.J. Islam, M.Z. Rahman, D. Zhu, Properties prediction of composites based on machine learning models: a focus on statistical index approaches, Mater. Today Commun. 38 (2024) 107659, https://doi.org/10.1016/J.MTCOMM.2023.107659.
[84] J. Zhang, G. Ma, Y. Huang, J. sun, F. Aslani, B. Nener, Modelling uniaxial compressive strength of lightweight self-compacting concrete using random forest regression, Construct. Build. Mater. 210 (2019) 713–719, https://doi.org/10.1016/J.CONBUILDMAT.2019.03.189.

[85] Y. Wu, Y. Zhou, Hybrid machine learning model and Shapley additive explanations for compressive strength of sustainable concrete, Construct. Build. Mater. 330 (2022) 127298, https://doi.org/10.1016/J.CONBUILDMAT.2022.127298.
[86] I.M. Nikbin, M.H.A. Beygi, M.T. Kazemi, J. Vaseghi Amiri, S. Rabbanifar, E. Rahmani, S. Rahimi, A comprehensive investigation into the effect of water to cement ratio and powder content on mechanical properties of self-compacting concrete, Construct. Build. Mater. 57 (2014) 69–80, https://doi.org/10.1016/j.conbuildmat.2014.01.098.
[87] P. Huang, K. Dai, X. Yu, Machine learning approach for investigating compressive strength of self-compacting concrete containing supplementary cementitious materials and recycled aggregate, J. Build. Eng. 79 (2023), https://doi.org/10.1016/j.jobe.2023.107904.
[88] H.A. Bulut, R. Şahin, Radiological characteristics of Self-Compacting Concretes incorporating fly ash, silica fume, and slag, J. Build. Eng. 58 (2022) 104987, https://doi.org/10.1016/J.JOBE.2022.104987.
[89] A.M. Zeyad, A. Almalki, Influence of mixing time and superplasticizer dosage on self-consolidating concrete properties, J. Mater. Res. Technol. 9 (2020) 6101–6115, https://doi.org/10.1016/J.JMRT.2020.04.013.
[90] K. Devi, P. Aggarwal, B. Saini, Admixtures used in self-compacting concrete: a review, Iranian Journal of Science and Technology - Transactions of Civil Engineering 44 (2020) 377–403, https://doi.org/10.1007/s40996-019-00244-4.
[91] M. Benaicha, A. Hafidi Alaoui, O. Jalbaud, Y. Burtschell, Dosage effect of superplasticizer on self-compacting concrete: correlation between rheology and strength, J. Mater. Res. Technol. 8 (2019) 2063–2069, https://doi.org/10.1016/j.jmrt.2019.01.015.
[92] V. Kannan, Strength and durability performance of self compacting concrete containing self-combusted rice husk ash and metakaolin, Construct. Build. Mater. 160 (2018) 169–179, https://doi.org/10.1016/J.CONBUILDMAT.2017.11.043.
[93] Y. Khodair, B. Bommareddy, Self-consolidating concrete using recycled concrete aggregate and high volume of fly ash, and slag, Construct. Build. Mater. 153 (2017) 307–316, https://doi.org/10.1016/J.CONBUILDMAT.2017.07.063.
[94] Z. Guo, J. Zhang, T. Jiang, T. Jiang, C. Chen, R. Bo, Y. Sun, Development of Sustainable Self-Compacting Concrete Using Recycled Concrete Aggregate and Fly Ash, Slag, Silica Fume, European Journal of Environmental and Civil Engineering, 2020, https://doi.org/10.1080/19648189.2020.1715847.
[95] N.C. Concha, M.A. Baccay, Effects of mineral and chemical admixtures on the rheological properties of self compacting concrete, Int. J. GEOMATE 18 (2020) 24–29, https://doi.org/10.21660/2020.66.9138.
[96] A. Mardani-Aghabaglou, M. Tuyan, G. Yilmaz, Ö. Ariöz, K. Ramyar, Effect of different types of superplasticizer on fresh, rheological and strength properties of self-consolidating concrete, Construct. Build. Mater. 47 (2013) 1020–1025, https://doi.org/10.1016/J.CONBUILDMAT.2013.05.105.
[97] S. Türkel, A. Kandemir, Fresh and hardened properties of SCC made with different aggregate and mineral admixtures, J. Mater. Civ. Eng. 22 (2010) 1025–1032, https://doi.org/10.1061/(asce)mt.1943-5533.0000107.
[98] L.A. Al-Jaberi, Effects of chemical admixtures on the rheological, fresh and hardened properties of self-compacting concrete, Academic J. for Eng. Sci. 1 (2019) 19–25. https://www.researchgate.net/publication/340298064_Effects_of_Chemical_Admixtures_on_the_Rheological_Fresh_and_Hardened_Properties_of_Self-Compacting_Concrete.
[99] T. Xie, M.S. Mohamad Ali, M. Elchalakani, P. Visintin, Modelling fresh and hardened properties of self-compacting concrete containing supplementary cementitious materials using reactive moduli, Construct. Build. Mater. 272 (2021) 121954, https://doi.org/10.1016/j.conbuildmat.2020.121954.
[100] M. Sahraoui, T. Bouziani, Effects of fine aggregates types and contents on rheological and fresh properties of SCC, J. Build. Eng. 26 (2019) 100890, https://doi.org/10.1016/J.JOBE.2019.100890.
[101] O. Almuwbber, R. Haldenwang, W. Mbasha, I. Masalova, The influence of variation in cement characteristics on workability and strength of SCC with fly ash and slag additions, Construct. Build. Mater. 160 (2018) 258–267, https://doi.org/10.1016/J.CONBUILDMAT.2017.11.039.
[102] D.K. Ashish, S.K. Verma, Determination of optimum mixture design method for self-compacting concrete: validation of method with experimental results, Construct. Build. Mater. 217 (2019) 664–678, https://doi.org/10.1016/j.conbuildmat.2019.05.034.
[103] M.S. Abo Dhaheer, M.M. Al-Rubaye, W.S. Alyhya, B.L. Karihaloo, S. Kulasegaram, Proportioning of self–compacting concrete mixes based on target plastic viscosity and compressive strength: Part I - mix design procedure, J Sustain. Cem. Based Mater. 5 (2016) 199–216, https://doi.org/10.1080/21650373.2015.1039625.